Installation and Commissioning of a Magnetic Compensation Loop and Booster Rectifier Circuit by Means of Reliable and Economically Efficient Bolted Joints

André Felipe Schneider[1], Donald P. Ziegler[2], Daniel Richard[3], Pascal Lavoie[4], René Trudel[5], Daniel Champagne[6], Timothée Turcotte[7], Alexandre Comeau[8], Alexandre Lamoureux[9], Dany Vaillancourt[10] and Levis Villeneuve[11]

1. Numerical Analysis Specialist – Aluminum, Hatch Ltd., Montreal, Canada
2. Program Manager – Modeling, Smelting Center of Excellence, Alcoa Technical Center, New Kensington, United States of America
3. Associate – Aluminum, Hatch Ltd., Saguenay, Canada
4. Consultant – Aluminum, Hatch Ltd., Deschambault, Canada
5. Operations Coordinator, Smelting Center of Excellence, Alcoa Deschambault Smelter, Deschambault, Canada
6. Consultant – Aluminum
7. Mechanical Engineer
8. Mechanical Engineer
9. Senior Numerical Analysist – Specialized Engineering Analysis & Design Hatch Ltd., Montreal, Canada
10. H&S Manager – Growth Project and Strategic Vision Manager, Alcoa Deschambault Smelter, Deschambault, Canada
11. Associate Project Manager, Hatch Ltd., Montreal, Canada

Corresponding author: andre.schneider@hatch.com

Abstract

ALCOA's Deschambault Smelter has been operating AP30 cells for more than 25 years, having crept its potline far beyond the original technology nameplate amperage. In order to validate the industrial performance of ALCOA's internally-designed technology upgrade enabling the operation of these pots at even higher amperage, a magnetic compensation loop and a new booster rectifier and circuit were installed in early 2017. Working in a brownfield environment where the magnetic field could exceed 13 mT, the Integrated ALCOA-HATCH Alliance Project Team decided to assemble the 3 km of total equivalent linear length of prefabricated busbars modules without welding, resorting only to bolted connections. While most of the design and installation effort was based on proven methods employed in past successful experiences, a new tightening procedure for the assembly of bolted joints was developed based on the insights gained from both bench testing and numerical analyses. Furthermore, the Project Team developed a new contact resistance testing protocol to validate the quality of each one of its 170 connections in pre-operational verifications without having the busbars energized. This helped to streamline the equipment commissioning, which was successfully completed under budget and on schedule, including a 48 h existing booster shutdown, but no potline outage. Finally, an economic analysis based on Project's total costs showed that the usage of reliable bolted connections can be cost-effective compared to traditional construction strategies using commercially available arc-welding methods subjected to the aforementioned conditions.

Keywords: Aluminum reduction cells, brownfield, busbars, magnetic compensation loop, bolted connections.

1 Introduction

The Alcoa Deschambault smelter was completed in 1992 and is built around a single potline of 264 AP30 cells featuring a booster section. The booster was built with the plant and included

prototype cells right from the first start-up. R&D and innovation are part of the Deschambault ongoing operational strategy, and the smelter is home to the Alcoa Center of Excellence (CoE) whose mission includes applied research, pilot testing, training for Alcoans around the world, and technical support to all Alcoa smelters.

The experience gained over more than 25 years of AP30 cells operation allied to ALCOA's CoE technical know-how allowed Alcoa Deschambault smelterto creep its potline far beyond the original technology nameplate amperage. In order to validate the industrial performance of an internally-designed technology upgrade enabling the operation of these pots at even higher amperage, a magnetic compensation loop (MCL) and a new booster rectifier and circuit were installed early 2017. The present article focuses on the design, installation and commissioning of these conductors.

2 New Magnetic Compensation Loop and Booster Circuits

Alcoa Deschambault's test section originally comprised 10 cells and is located in the B room upstream of the smelter's 3/4 passageway. A first retrofit enabled the inclusion of two additional pots (B110 and B111) in the boosted segment of the potline, which was then fed by a 22 kA GE booster rectifier. The positive booster circuit, located on the "outside" (tapping end) and running in a direction opposed to that of the potline, provided partial magnetic compensation to these pots.

By 2015, the existing booster rectifier was getting close to the end of its service life and would have to be either retrofitted or replaced. Magnetohydrodynamics studies performed by CoE indicated that a magnetic compensation loop (MCL) would be required to allow for stable operation of the next pot generation to be field-trialed at higher amperage. Furthermore, to realistically emulate the future magnetic environment to be experienced by the pots once the current of the whole potline has reached the target amperage level, the original booster circuit routing had to be modified.

An option analysis performed by the Integrated ALCOA-HATCH Alliance Project Team indicated that the most viable scenario would be to install a brand-new booster rectifier to feed the test section while repurposing the original 22 kA rectifier to feed the MCL prototype. The new service conditions of the existing rectifier at a significantly lower voltage drop would extend the aging equipment's life span, and therefore reduce the capital expenditure involved in the trials.

2.1 Layout

Aiming to generate a vertical magnetic field bias on the test pots similar to that of a mid-section pot at the target increased amperage, the positive branch of the new booster circuit was relocated to the tap end (TE) of the opposite pot row, crossing under two cells outside of the testing section, namely A121 and B121 – see Figure 1. Due to the limitations of the original booster rectifier, the MCL prototype routing employs 3 turns to meet the process requirements since these conductors had to be installed in the small aisle (duct end, DE) in close proximity to each other.

The total linear length of both circuits is 3 km. As a strategy to reduce the aluminum purchasing costs, the temporary potline startup bridge – which was stored in the 3/4 passageway since the smelter's start-up – was modified and its busbars were used for both the new booster circuit and the MCL prototype.

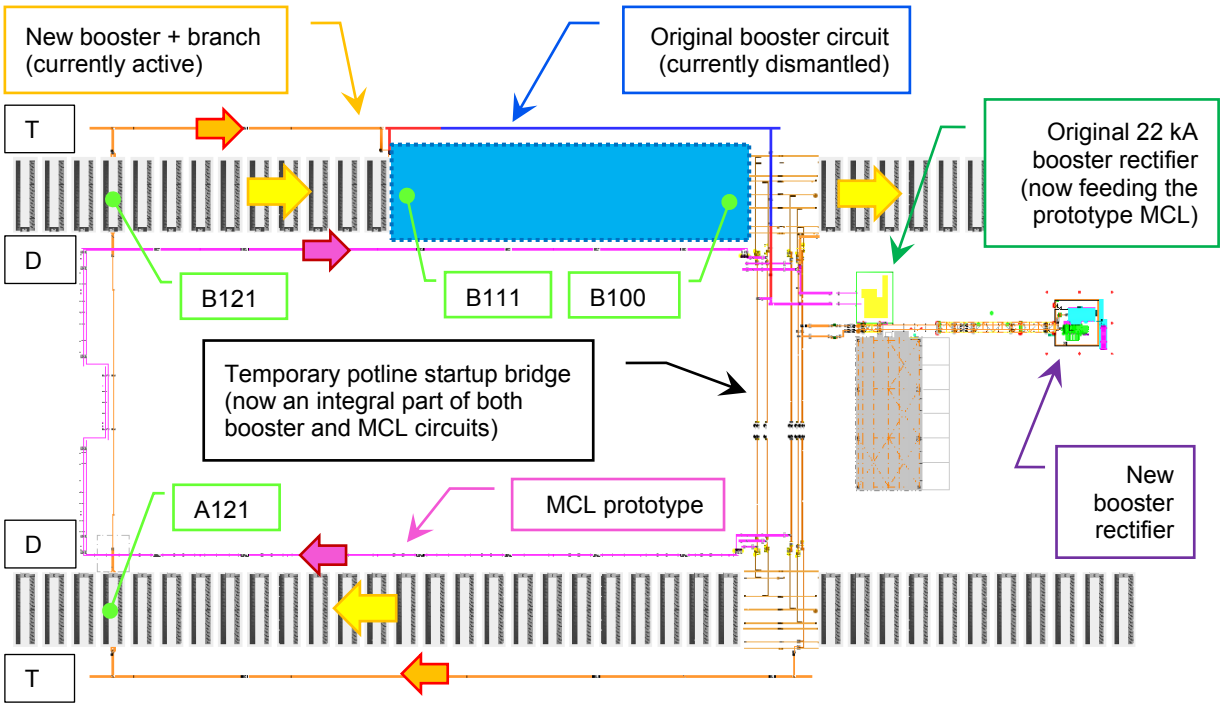

Figure 1. New booster and MCL circuits layout.

These features involving three separate circuits (booster, MCL, potline) have implications on the definition of the electrical insulation and protection design philosophy, the detailed design of the busbar assemblies and their supports as well as the selection of the method for the on-site joining of conductors.

3 Electrical Insulation and Protection

The addition of the new booster and MCL circuits introduced new electrical risks, such as:

- Bridging between MCL and ground (ground) potentials when manually opening the potroom louvers or accidentally touching an exposed metallic structural member of the building;
- Bridging between MCL and pot potential when working with a (long) metallic tool in the basement, DE;
- Bridging between 2 adjacent loops of the MCL;
- Bridging between ground and either pot B111 or MCL potentials in the inner yards, especially when operating a vehicle close to the 4/4 passageway access ramp or the new booster rectifier bay;
- Bridging between ground and either MCL or boosted pots potentials when working in the 3/4 passageway at the basement level.

A systematic risk assessment was performed to determine the appropriate approach to mitigating the risks. While some were mitigated simply by restricting the access to certain areas (administrative control), others required special electrical protection and insulation elements – see, for instance, Figure 2, where suspended segments of both new circuits had to be covered with insulating panels.

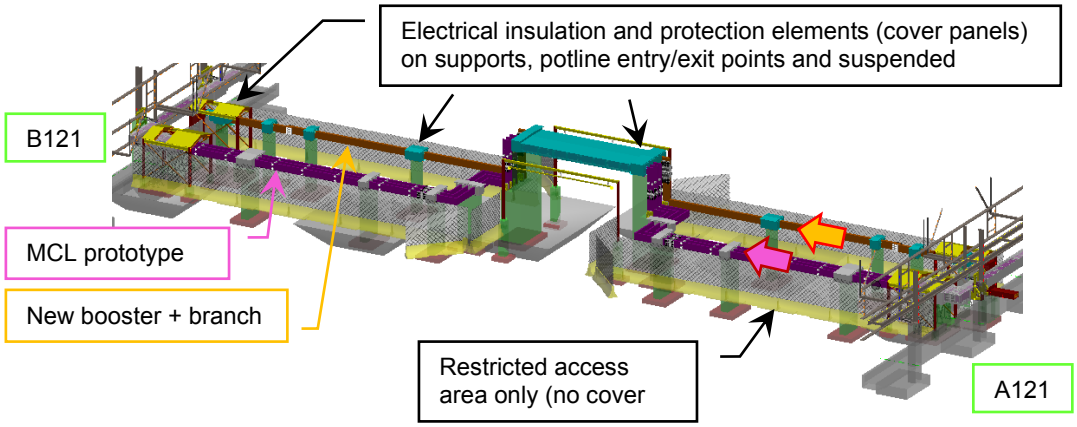

Figure 2. Electrical protection and insulation elements at the inner yard near the 4/4 passageway access ramp.

Adjacent turns of the typical small aisle MCL assembly had to be insulated from one another by insulating plates while the whole busbars bundle was covered with insulating panels, Figure 3. Note that the metallic supports in this sector include 2 layers of electrical insulators given that they are anchored directly to potroom structure (*i.e.*, at ground potential).

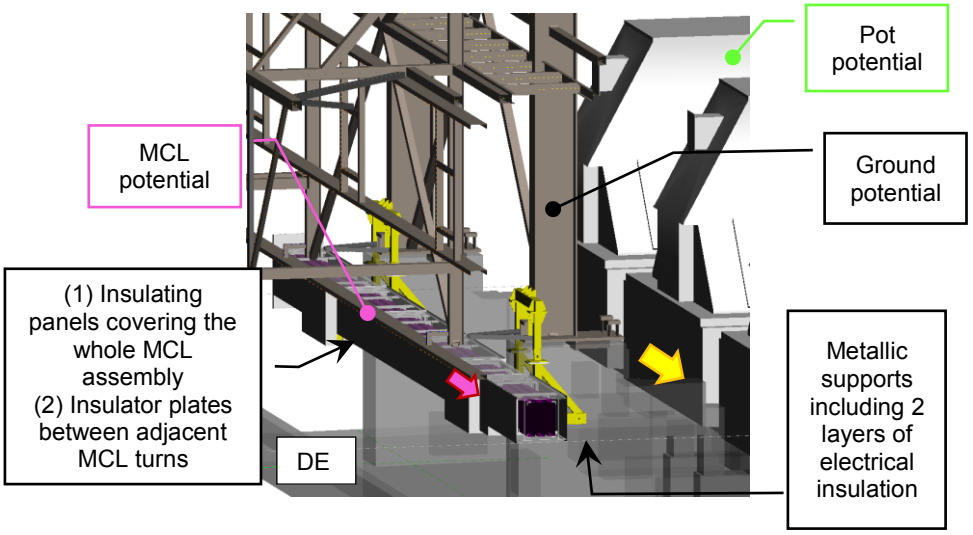

Figure 3. Electrical protection and insulation for the typical small aisle MCL assembly

Special attention was given to the risk of bridging the potentials of pots B111 and either A121 or B121, should one of the latter two tap out.

3.1 Precast Concrete Culverts

Precast concrete culverts were employed to mitigate the risk of molten metal spillage over the new booster circuit segments in the vicinity of pots A121 and B121, according to Figure 4.

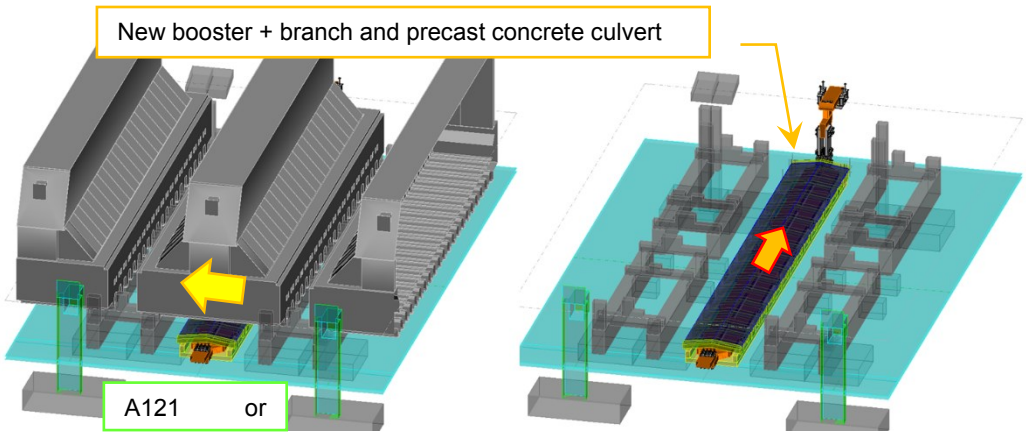

Figure 4. New booster positive circuit near cells A121 and B121.

Since these busbars segments are enclosed, thereby limiting their convective and radiative cooling capacity with the environment, additional design considerations were given to these sections of the booster circuit. As a first precaution, the busbar cross-sectional area was doubled inside the culverts to reduce the local current density and ohmic heat generation within the conductors. In addition to this, the culverts were designed with side openings to allow air circulation and minimal convective cooling of the enclosed busbars. Lastly, it was deemed necessary to conduct a computational fluid dynamics (CFD) analysis of these booster busbar circuit segments to validate their design. This exercise is summarized in the following paragraphs.

Since both enclosed booster sections are essentially identical, a single CFD model was necessary. The calculation domain comprised the pot located above the culverts and one half-pot on each side, totalizing two full pots. It included the horizontal and vertical booster busbar segments of interest, busbar spacers and electric insulators, the culvert, nearby civil works and structures, the pot shells extending below the operation floor, simplified pot-to-pot conductors and the volume of air bounded by the following limits: the basement floor, the central planes of both neighboring pots, the basement ceiling and basement side ventilation openings.

The model was implemented and solved using ANSYS FLUENT® V14.1. A detailed description of the employed mathematical model, modeling settings and strategy is outside the scope of this paper. The key modeling settings, parameters and boundary conditions, are summarized below:

- A steady-state condition (flow and temperature fields) was assumed to prevail;
- Turbulence was modeled using the k-epsilon realized model;
- Air was treated as an ideal gas (locally incompressible), with density and other transport properties prescribed as functions of temperature;
- Buoyancy forces were modeled by means of locally variable air density;
- The electric potential and current problem was solved within the busbars. The resulting current density field was used to evaluate local ohmic heat generation;
- The far-field (exterior) ingress air temperature was set to 35 °C, in accordance with the design criteria;
- A fixed volumetric flow rate of ingress air was prescribed at both building side openings. A predetermined fraction (based on site data and previous modeling efforts) of this incoming flow rate was diverted to the Claustra wall enclosures, while the portion remaining in the basement level exited through the pot side gratings;

- The prescribed total air ventilation flow rate entering through the building side openings is based on available site measurements and reflect minimum values prevailing in summer conditions (opened side panels). This conservative value was kept constant for all cases;
- Previously measured pot shell and pot-to-pot conductor temperatures were prescribed as boundary conditions at the corresponding locations;
- Although spatially-cyclic boundary conditions would strictly be preferable along the lateral limits of the domain (neighboring pot central planes), symmetry conditions, which favor the rate of convergence of the solution process, were deemed sufficiently accurate and were prescribed at these locations.

In addition to preliminary grid-independence studies, a total of five main cases were solved to study multiple possible distributions of the ingress air flow rate between the tap and duct side openings. This approach was deemed to be a conservative and cost-effective way of studying multiple ingress air flow rate distributions which could be induced by various wind conditions without resorting to large-scale, computationally expensive plant-wide external CFD models. These cases are listed in Table 1 below.

Table 1. List of Solved Cases for Culvert Busbar CFD Model.

Case	Ingress air flow rate distribution	
	Tap end (%)	Duct end (%)
1	50	50
2	25	75
3	75	25
4	0	100
5	100	0

The key numerical predictions included: the volume-average and maximum horizontal busbar temperatures (within culverts), the maximum vertical busbar temperatures (outside culverts), the maximum culvert temperature along its outer and inner surfaces, and the maximum spacer and electric insulator temperatures. These results were used to ensure that all design criteria, such as the thermal limits of key components, were respected. A sample image of a simulation is provided below in Figure 5.

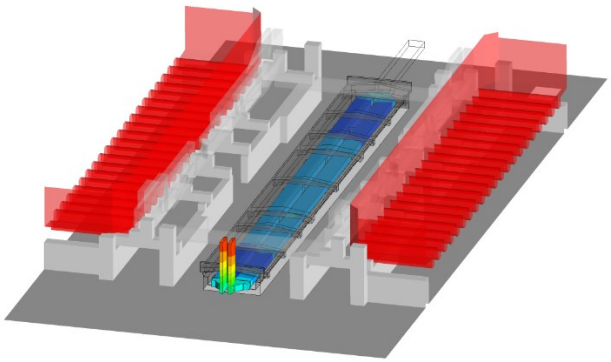

Figure 5. Sample results for Case 1, busbar temperature levels illustrated (central pot outer shell removed from image for clarity purposes).

4 Busbar Supports Design

The main electrical risks identified in Section 3 were also considered for the detailed design of busbar supports (Figure 6). The fault currents for each case were obtained by a Matlab®/Simulink®-based transient electrical analysis considering the characteristics of the

electrical equipment and the properties of the circuits. The resulting magnetic fields and Lorentz forces acting on the conductors were then obtained by an in-house integral method, briefly discussed below.

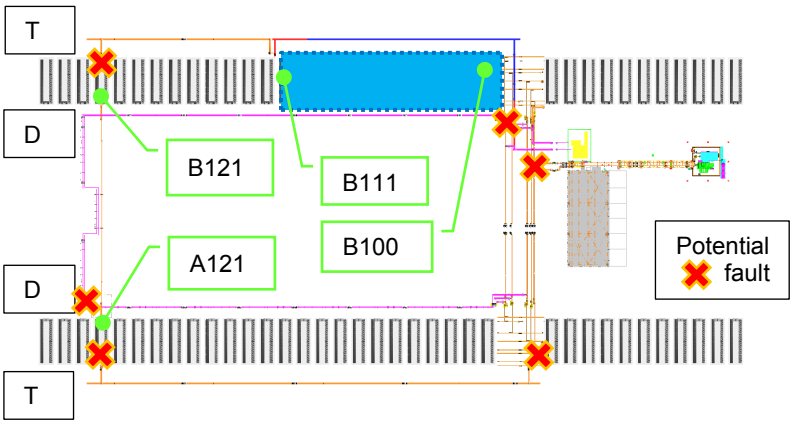

Figure 6. Potential short-circuit scenarios considered during busbar supports design.

4.1 In-house Biot-Savart Numerical Method

An in-house numerical method was programmed using Matlab® to predict the magnetic field emanating from conductors and the resulting Lorentz forces acting on their neighbors.

The implemented mathematical model stems from the well-known Biot-Savart law which is readily available in the literature. The approach followed by the numerical method is described next. Each conductor in the provided ensemble can be considered as both an "emitter" (inducing a magnetic field) and a "receiver" (incurred Lorentz force due to local magnetic and current density fields). The method first discretizes each conductor over their cross-section into a group of line-elements emitters, each spanning the full length of the linear (straight) conductor, in accordance with the settings provided by the user (ex: 5 x 3 elements over the conductor cross-section height and width, respectively). Then, each conductor is discretized over their cross-section and along their longitudinal direction into receiver elements, again as instructed by the user. This discretization approach is illustrated in Figure 7.

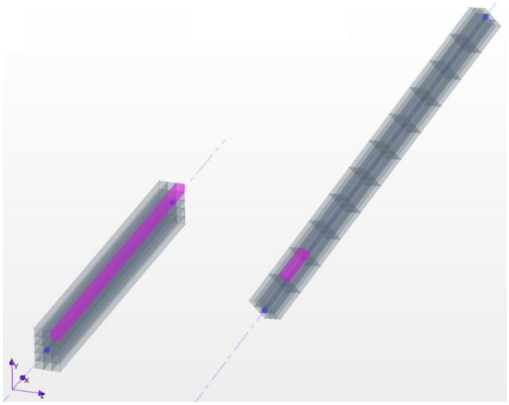

Figure 7. Schematic of a line-element emitter and a receiver element in a discretized conductor pair (highlighted to the left and right, respectively).

In accordance with the superposition principle, the individual contributions of each line-emitter to the magnetic field at the receiver element centroids are cumulatively evaluated and stored. Once the contributions of all line-emitter elements have been computed, the method yields an

evaluation of the magnetic field over all receiver elements and their parent conductors. The use of line-element emitters greatly reduces the overall computational effort, as the emitter conductors are not discretized along their longitudinal direction, thereby reducing the total number of emitter-conductor pairs and associated calculations. Naturally, depending on the problem geometry and conditions, sufficient discretization of the conductors is needed to attain accurate solutions. Consequently, the user must perform discretization level verifications analogous to mesh-independence studies conducted with other element-based or control-volume based numerical methods.

Lastly, the method computes the Lorentz forces using local (centroid-stored) values of the magnetic field and current density. These elemental forces are then agglomerated over cross-sections and full conductors as required to yield the total forces required for further mechanical and structural analyses. It is key to mention that this in-house code also allows the evaluation of magnetic field at locations other than conductors (ex: mesh of points, etc.), regardless of the orientation of the conductors in space. Prior to being used, this code was validated using available analytical solutions for three test problems: i) an infinitely-thin, parallel conductor pair, ii) a circular coil and iii) a parallel conductor pair of finite dimensions located close with respect to each other. The use of this in-house Biot-Savart method for the currently-discussed project is described next.

4.2 Mechanical Reactions on Busbar Supports

The electromagnetic forces obtained for the potential short-circuit scenarios with the in-house Biot-Savart method were then transferred to a Finite Element (FE) model – described in detail by [1] – to obtain the resulting reactions at the supports, considering also gravity and thermal expansion. The frequent changes in direction found along the new booster circuit and MCL paths results in loads that differ substantially from that of the infinitely long parallel conductors approximation. For example, busbar uplift was predicted in some circumstances due to upward force of considerable magnitude near the connections of horizontal and vertical busbar segments, as per Figure 8. Consequently, special bracing was designed and installed at specific supports.

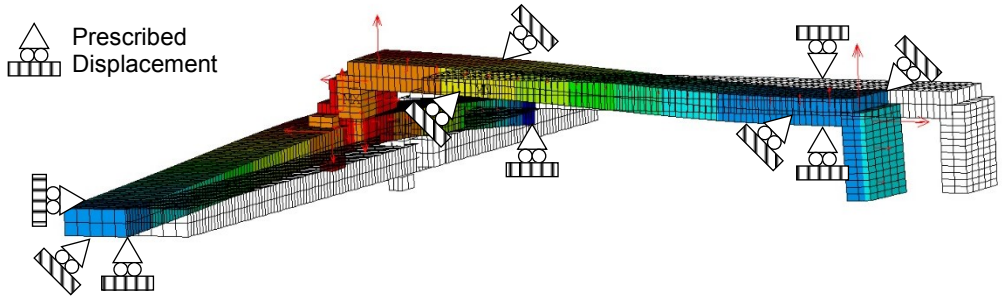

Figure 8. Busbar uplift resulting from Lorentz forces

5 On-Site Busbar Installation

As previously mentioned, process requirements and design-related circuit features influenced the selection of the joining method for the *in situ* connection of the prefabricated busbar assemblies:

- Exothermic welding (CAD welding): the available room between the three adjacent segments of the typical small aisle MCL prefabricated assembly prevented the mounting of the moulds. Alternatively, each turn might have been individually

positioned and welded on site, substantially increasing total installation time and cost. Also, the tailor-made nature of the new circuits (especially at the 3/4 passageway, refer to Section 2.1 and Figure 1) led to a significant number of special joint configurations, which would in turn considerably increase the mould fabrication costs;

- Electroslag welding (ESW): the measured magnetic flux density at the typical small aisle MCL location could exceed 13 mT, which would hinder the welding process at the time the *in-situ* busbars joining technique was being selected. Once again, significant number of moulds would be required to account for the different joint configurations;
- Conventional arc-welding: the magnetic field in the small aisle would require the employment of specifically-trained welders and the use of magnetic shielding devices.

Successful past experiences [2, 3] encouraged the Integrated ALCOA-HATCH Alliance Project Team to assemble on site the prefabricated busbars by bolted connections. While not straightforward, this solution allows for considerable design freedom since it can be adapted to any busbar configuration, it does not rely on the know-how of a specific (sole source) vendor nor any kind of special equipment, and its installation had been proven feasible in the presence of strong magnetic fields.

While both the design and installation effort were largely based on proven methods (such as the employment of *Belleville* washer stacks and *in situ* drilling/machining of existing conductors), a new tightening procedure for the assembly of bolted joints was developed based on the insights gained from both bench testing and numerical analyses.

5.1 Tightening of Bolted Joints with Spring Washer Stacks on Both Ends

Schneider *et al.* reported [3] that a calibrated hydraulic torque wrench could be used to tighten bolted joints including *Belleville* washer stacks. It is important to stress, however, that the series of tightening tests performed at that time included only joints with spring washers installed on only one end of a given tie-rod while the torque was applied on the opposite extremity where the nut is sitting on a standard, flat washer. Bench tests also confirmed that standard friction coefficient values are obtained if the joint is tightened from the nut end, that is, with the torque wrench installed on a nut sitting directly on static flat surface (without spring washers).

However, an arrangement with 2 stacks in series of *Belleville* washers was designed for the project due to the high expected temperatures and consequently a large busbar-to-tie rod differential thermal expansion to be absorbed by the joints of the 3/4 passageway bypass bridge. In fact, even though the temporary potline startup bridge was modified and incorporated into the new circuits, it still required to act as an emergency bypass bridge in case of a major potline failure. With one stack installed on each end of the tie-rod, the hydraulic tool would have to act on the *Belleville* end – therefore, the above-described procedure did not apply. A new series of bench tests was thus performed to assess the impact of tightening of bolted joint on the spring washer stack end, as shown in Figure 9.

It was found that the grease film applied between spring washers decreases significantly the effective friction coefficient of the assembly when tightening the joint from the spring washer stack side, allowing the disks to rotate with respect to each other. The unintended consequence is a significant increase in bolt pretension for a prescribed torque.

The impact of potentially overloading the tie-rods on the joint's stability was theoretically assessed using an axisymmetric thermo-elastoplastic analysis of the tightening operation – see Figure 10. A non-linear stress (σ)-strain (ε) curve representing the spring washers stack force-deflection behavior from rest to flat position was implemented based on the experimental data.

The evolution of the different material properties with temperature was also considered, including a non-linear σ-ε curve for the aluminum.

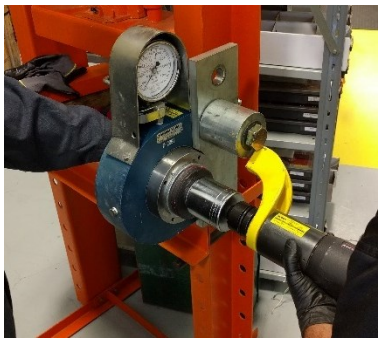

Figure 9. Bench testing campaign – tightening of a bolted joint on the *Belleville* washer stack end.

First, an overload pretension representative of the experimental results, was prescribed to the tie-rod. Then 3 complete summer operation-to-winter stoppage cycles were simulated, assuming that the bolted joint's temperature increased by 50 °C during each operation regime to represent the pessimistic degradation of the joint quality. Numerical results indicate that even if the resulting contact pressure reduces at the end of each thermal cycle (due to increasing permanent deformation of aluminum conductors), it does not drop below 5 MPa indicating that there would be no risk of interfacial opening (and, consequently, of air infiltration leading to joint quality degradation) during a wintertime shutdown. In a nutshell, the bolted joint design is actually more robust than initially believed by the Project Team.

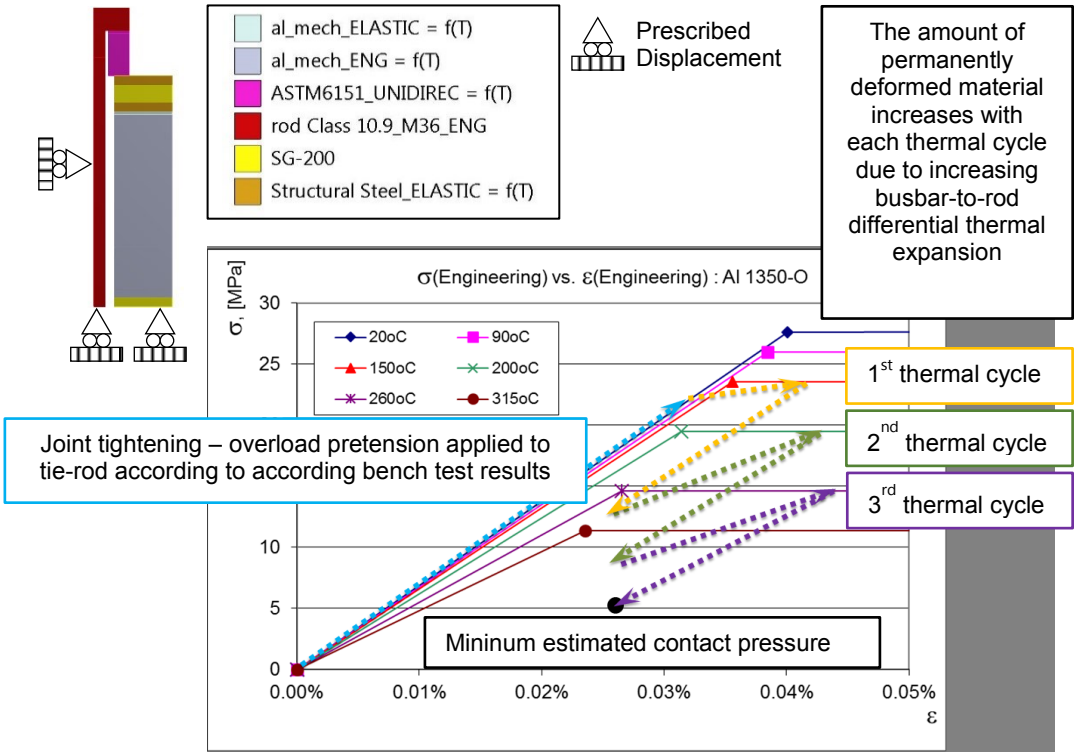

Figure 10. Axisymmetric FE analysis of a bolted joint including the non-linear force-displacement behavior of a stack of *Belleville* washers.

Nevertheless, it is the authors firm belief that a high-current bolted joint should be designed and assembled according to the principles enumerated by [3], including to keep the spring washer stacks within the recommended deflection range at all times. Therefore, the tightening procedure originally employed by [3] was modified by the Project Team to ensure that a consistent friction value is always considered when designing and assembling a bolted joint. The simplest way to achieve this is to apply the tightening torque to a nut sitting directly on static, flat surface (*e.g.*, without spring washers).

5.2 Flexible Braided Joints

Due to spacing constraints, the joining of typical small aisle MCL assemblies with 3 adjacent busbar segments was performed by employing tin-plated copper braided flexible connectors, similar to those shown in Figure 11. Flexible arrangements based on these components were systematically used in the design process, except at the 3/4 passageway emergency bypass bridge.

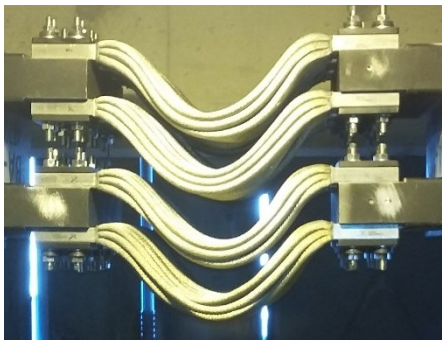

Figure 11. Example of a flexible joint assembled with tin-plated cooper connectors (new booster positive circuit).

Experience suggests that the quality of the plating process has a major impact on the busbar-to-braided connector ferrule interface contact resistance (R_{ctc}). Therefore, a laboratory testing campaign was performed to validate the performance of the proposed designs with the components of the selected braided flexible vendor. Experimental results met the Project's design criteria.

5.3 Bolted Joints Quality Assurance

Given the important number of bolted joints included in the Project, it was decided to validate their quality briefly after tightening to reduce commissioning time. A rigorous quality control system was put in place, where the connections were assessed by means of overall resistance measurements performed with a Raytech's Centurion II® micro-ohmmeter (resolution of 0.01 μΩ at 200 A). Considerable attention was given in order not to affect the readings due to induced voltage in the reading cables.

The average R_{ctc} of each joint was derived by subtracting its intrinsic theoretical resistance (obtained from a purely electrical FE analysis) from the total measured value, analogous to the methodology described by [4] – individual R_{ctc} validation templates were produced for each unique joint type in order to ensure that a standardized, consistent assessment procedure was followed by the installation contractor at all times.

Figure 12 below shows the estimated R_{ctc} for all the bolted joints assessed at the Pre-Operational Verifications (POV) phase, prior to system's start-up: note that while the design criterion of 0.030 $\mu\Omega m^2$ agrees with [3], the acceptable limit was reduced to 0.040 $\mu\Omega m^2$ (instead of 0.060

$\mu\Omega m^2$). A joint that was deemed unacceptable had to be opened, cleaned, prepared and tightened anew: only 3 joints out of 170 (or less than 2 %) had to be reworked.

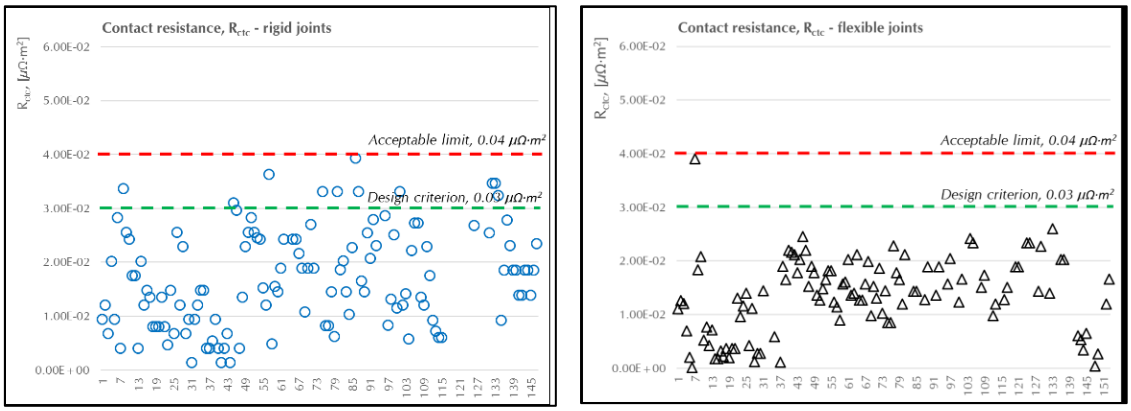

Figure 12. Estimated R_{ctc} for both rigid (left) and flexible (right) bolted connections.

5.4 Existing Booster Rectifier Shutdown and System Commissioning

Similar to the bolted joints quality control approach, the electrical insulation level of the entire installation was assessed by resistance measurements employing a mega-ohmmeter prior to existing booster rectifier shutdown. The carefully planned and executed construction and POV strategies allowed this critical Project phase to be safely completed within 48 h, including:

- Interrupting the connection between the existing 22 kA booster rectifier and cell B111;
- Connecting new booster positive to cell B111;
- Closing the last MCL-to-existing 3/4 passageway temporary potline startup bridge bolted connection.

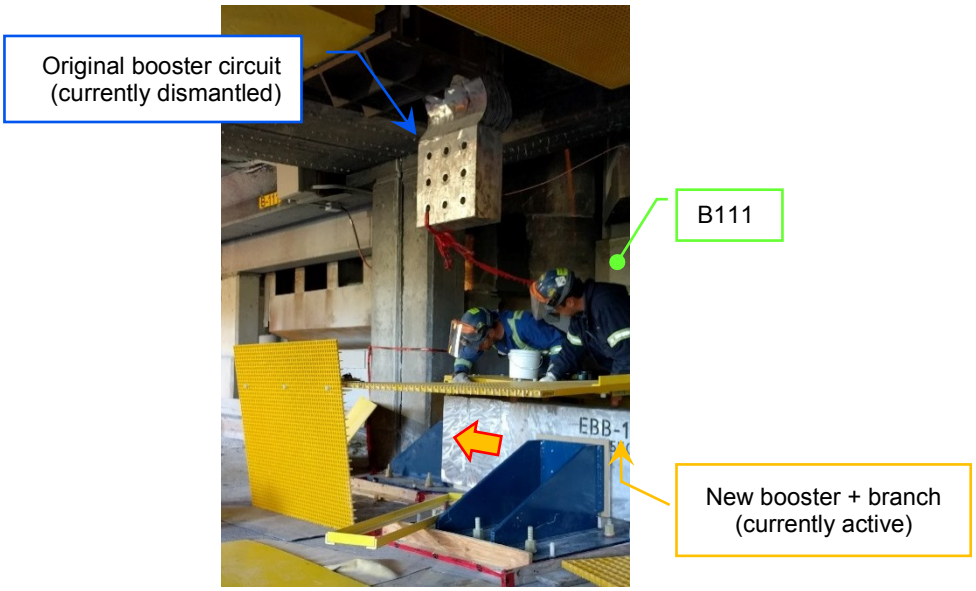

Figure 13. Connection of the new booster positive branch to pot B111.

Two busbar temperature measurements campaigns were completed to ensure that the bolted joints assembled by the Project were functioning properly: the first in the day following the circuits startup and the second, 2 months later. All recorded data indicated that the joints (and busbars) were running within expected temperature rises above ambient.

The system was finally commissioned under budget and on schedule and has been operating in a consistent, stable manner for more than 12 months.

5.5 Economic Performance of the Adopted Construction Strategy

Project's total figures (including the extensive POV effort, Section 5.3) were used to estimate the costs of assembling a new MCL with a total linear length of 1.8 km of prefabricated conductors by means of bolted joints –. The exercise also included the comparison with the costs involved in erecting the same circuit by means of a proprietary arc-welding technology, capable of achieving good quality joints when subjected to magnetic fields as intense as those described in this article.

Relative calculated figures for both options are respectively presented in Table 2 and Table 3, considering the bolted joints one as the reference case. Note that these estimates are focused on the supply and the installation of busbars only, *i.e.*, costs regarding electrical protection and insulation elements, supports and others are excluded. Both estimates are assumed to be of budget-level quality, accurate within ± 30 %.

Table 2. Relative installation costs for the *in situ* assembly of a new MCL by means of bolted connections.

On-Site Joining by Means of Bolted Connections, Including Copper Braided Flexibles Every 36 m				
Item	**Qty, [-]**	**Total Relative Supply Cost, [-]**	**Total Relative Labor Cost, [-]**	**Total Relative Cost, [-]**
Supplying & on-Site Handling of Prefabricated Busbar Assemblies	70	23.8%	38.4%	62.2%
Tightening of Busbar-to-Busbar Rigid Joint (Including Hardware Supplying & POV Testing)	30	2.0%	2.2%	4.2%
Supplying of Tin-plated Copper Braided Flexible Connectors	396	26.5%	-	26.5%
Tightening of Braided Connector-to-Busbar Flexible Joint (Including Hardware Supplying & POV Testing)	33	4.7%	2.4%	7.1%
			Total	100.0%

Table 3. Relative installation costs for the *in situ* assembly of a new MCL by means of a proprietary arc-welding process.

On-Site Joining by Means of a Proprietary Arc-Welding Process, Including Laminated Aluminum Flexibles Every 54 m				
Item	**Qty, [-]**	**Total Relative Supply Cost, [-]**	**Total Relative Labor Cost, [-]**	**Total Relative Cost, [-]**
Purchasing of Prefabricated Busbar Assemblies (Including Laminated Aluminum Flexibles)	70	42.1%	-	42.1%
On-Site Welding & Handling of Prefabricated Busbar Assemblies	1	-	187.8%	187.8%
			Total	229.9%

It can be seen from the data above that considerable savings can be obtained when considering the usage of bolted connections for the *in situ* joining of prefabricated conductors in complex brownfield environments with intense magnetic fields.

It is important to stress, however, that bolted connections lead to voltage drops larger than those obtained by welded joints and, therefore, the associated energy costs must be taken into account in order to appropriately calculate the Project's economics.

6 Conclusions

An Integrated ALCOA-HATCH Alliance Project Team successfully installed an equivalent 3 linear km of prefabricated busbars modules without welding, resorting only to bolted connections. While most of the design and installation effort was based on proven methods, a new tightening procedure for the assembly of bolted joints was developed based on the insights gained from both bench testing and numerical analyses.

The addition of the new booster circuit and prototype MCL introduced new electrical risks to the smelter which were managed by employing several mitigation strategies, including the employment of precast concrete culverts to prevent the short-circuiting of different pot-potentials due to molten metal spillage on the new booster positive circuit. This and other potential short-circuit scenarios were taken into account when designing the busbar details and their supports.

A new contact resistance testing protocol was devised to validate the quality of each one of the 170 connections in POV phase. Likewise, the electrical insulation levels of the entire installation was assessed prior to system's startup. This helped to streamline the equipment commissioning, which was successfully completed under budget and on schedule, including a 48 h existing booster shutdown, but no potline outage.

Finally, an economic analysis based on Project's total costs showed that the usage of reliable bolted connections can be cost-effective compared to traditional construction strategies using commercially available arc-welding methods when working on complex brownfield environments subjected to intense magnetic fields.

7 References

1. André Felipe Schneider *et al.*, A Thermal-mechanical approach for the design of busbars details, *Light Metals* 2013, 829-834.
2. Daniel Champagne, Donald P. Ziegler, Andre Felipe Schneider, and Daniel Richard., Busbar circuit design and installation for boosting already boosted pots, *Light Metals* 2010, 479-484.
3. André Felipe Schneider et al., Retrofit of damaged corner risers by means of bolted connections, *Light Metals* 2017, 731-738.
4. David Molenaar and T. Kilpatrick, Anode rod to beam contact, *Light Metals* 2014, 511-516.